



OPEN

D,L-Methadone causes leukemic cell apoptosis via an OPRM1-triggered increase in IP3R-mediated ER Ca²⁺ release and decrease in Ca²⁺ efflux, elevating [Ca²⁺]_i

JungKwon Lee^{1,2}, Jesusa L. Rosales¹, Hee-Guk Byun² & Ki-Young Lee^{1✉}

The search continues for improved therapy for acute lymphoblastic leukemia (aLL), the most common malignancy in children. Recently, D,L-methadone was put forth as sensitizer for aLL chemotherapy. However, the specific target of D,L-methadone in leukemic cells and the mechanism by which it induces leukemic cell apoptosis remain to be defined. Here, we demonstrate that D,L-methadone induces leukemic cell apoptosis through activation of the mu1 subtype of opioid receptors (OPRM1). D,L-Methadone evokes IP3R-mediated ER Ca²⁺ release that is inhibited by OPRM1 loss. In addition, the rate of Ca²⁺ extrusion following D,L-methadone treatment is reduced, but is accelerated by loss of OPRM1. These D,L-methadone effects cause a lethal rise in [Ca²⁺]_i that is again inhibited by OPRM1 loss, which then prevents D,L-methadone-induced apoptosis that is associated with activation of calpain-1, truncation of Bid, cytochrome C release, and proteolysis of caspase-3/12. Chelating intracellular Ca²⁺ with BAPTA-AM reverses D,L-methadone-induced apoptosis, establishing a link between the rise in [Ca²⁺]_i and D,L-methadone-induced apoptosis. Altogether, our findings point to OPRM1 as a specific target of D,L-methadone in leukemic cells, and that OPRM1 activation by D,L-methadone disrupts IP3R-mediated ER Ca²⁺ release and rate of Ca²⁺ efflux, causing a rise in [Ca²⁺]_i that upregulates the calpain-1-Bid-cytochrome C-caspase-3/12 apoptotic pathway.

Acute lymphoblastic leukemia (aLL) is a malignancy of B- or T-lymphoblasts that mostly affects children¹. It comprises over a quarter of all pediatric cancers and causes most of the cancer deaths among children². While newer targeted therapies for aLL have been developed, their effectiveness is enhanced when used in combination with chemotherapy, which remains to be the major treatment for aLL. Chemotherapy drugs kill leukemic cells by inducing apoptosis through blockade of nucleic acid synthesis or direct targeting of DNA, interfering with protein synthesis or inhibiting mitosis, respectively³. Recently, the synthetic opioid, D,L-methadone, was hailed as an antineoplastic agent, particularly for leukemia^{4–6} and glioblastoma^{4,7}. It was also shown to sensitize leukemia^{5,6} and glioblastoma cells⁷ to doxorubicin treatment.

D,L-Methadone was first developed for the stabilization and maintenance of patients suffering from addiction to other opioids such as heroin, oxycodone or fentanyl⁸. It is also used as an analgesic for the management of chronic pain such as in cancer⁹. The pharmacological effects of D,L-methadone have been associated with its interaction with Fas cell death receptors¹⁰, toll-like receptors¹¹, 3β4 nicotinic acetylcholine receptors¹² and N-methyl-D-aspartate receptors¹³, but primarily with opioid G-protein-coupled receptors (GPCRs)¹⁴. Thus far, four types of opioid receptors have been cloned: the classical mu (μ), kappa (κ) and delta (δ) opioid receptors, and the nociceptin/orphanin FQ receptor (aka opioid receptor-like receptor)¹⁵. Three subtypes of the mu opioid receptor have been proposed: mu1, mu2, and morphine-6β-glucuronide (M6G)¹⁶. Although these opioid receptor subtypes have high homology, each receptor poses distinct localization, agonist selectivity, and transcriptional regulation¹⁵.

¹Department of Cell Biology and Anatomy, Arnie Charbonneau Cancer, Alberta Children's Hospital Research Institutes, Cumming School of Medicine, University of Calgary, Calgary, AB T2N 4N1, Canada. ²Department of Marine Biotechnology, Gangneung-Wonju National University, Gangneung, South Korea. ✉email: kylee@ucalgary.ca

Activation of opioid GPCRs induces conformational change in the receptor that facilitates the exchange of GDP for GTP on G_{α} , leading to uncoupling from $G_{\beta\gamma}$ ¹⁷. Uncoupled GTP-bound G_{α} and $G_{\beta\gamma}$ dimer regulate diverse physiological functions including apoptosis⁵ through stimulation of their downstream effectors such as cyclic adenosine monophosphate (cAMP) and Ca^{2+} ¹⁸. As with other GPCRs, opioid receptors bind to G_{α} subunits, including members of the $G_{\alpha i/o}$ family^{19,20}. $G_{\alpha i/o}$ subunit activation by opioid receptors has been shown to decrease intracellular cAMP levels^{21,22} induced by the adenylyl cyclase activator, forskolin²³. On the other hand, the $G_{\beta\gamma}$ subunit mediates opioid-induced stimulation of phospholipase C β (PLC β); none of the pertussis toxin (PTX)-sensitive G_{α} subunits can activate PLC β by themselves^{24,25}. In neuroblastoma cells, $G_{\beta\gamma}$ subunit activation of PLC β is linked to opioid-induced ER Ca^{2+} release²⁶. This is consistent with the finding that opioid receptor stimulation by opioids causes a surge in $[Ca^{2+}]_i$ in leukocytes^{22,27}, pituitary²⁸ and neuroblastoma cells²⁶ through $G_{\beta\gamma}$, which is now recognized to stimulate PLC, which in turn cleaves phosphatidylinositol 4,5-bisphosphate (PIP2) into diacylglycerol (DAG) and inositol 1,4,5-trisphosphate (IP3). IP3 binds to the IP3 receptor (IP3R), triggering the opening of the IP3R Ca^{2+} channels and release of Ca^{2+} from internal stores to the cytosol. Along these lines, it is not surprising that mu opioid receptors have been implicated in intracellular Ca^{2+} homeostasis in neuroblastoma²⁹ and pituitary cells²⁸. Thus, as with other receptors that exploit $G_{\alpha i}$ and $G_{\beta\gamma}$ for signal transduction, opioid GPCRs act via the adenylyl cyclase/cAMP- and Ca^{2+} -mediated pathways.

The finding that D,L-methadone causes opioid receptor-mediated cAMP downregulation in leukemic cells⁵ is consistent with the fact that $G_{\alpha i}$ blocks adenylyl cyclase activity, causing reduced intracellular [cAMP]¹⁷ that leads to apoptosis through activation of caspases³⁰. While D,L-methadone is characterized as an opioid receptor agonist⁵, the specific opioid receptor target and molecular mechanisms of D,L-methadone-induced leukemic cell death remains to be defined.

By unbiased genome-wide retroviral RNAi screening and knockdown studies, we recently identified the mu1 subtype of opioid receptors (opioid receptor mu1: OPRM1) as a novel resistance biomarker for L-asparaginase, a fundamental component of chemotherapy regimens for aLL³¹. We found that OPRM1 is required for L-asparaginase to induce apoptosis and that loss of OPRM1 leads to L-asparaginase resistance³¹. This finding together with those described above prompted us to investigate whether D,L-methadone specifically targets OPRM1 to induce leukemic cell apoptosis, and if so, determine whether OPRM1-mediated D,L-methadone-induced apoptosis occurs through aberrations in $[Ca^{2+}]_i$.

Using POETIC2 aLL cells (*) stably infected with retrovirus carrying an empty pRS vector (*+pRS) or pRS-shOPRM1 (*+pRS-shOPRM1), we demonstrate that D,L-methadone induces leukemic cell apoptosis by targeting OPRM1 to increase Ca^{2+} release from the endoplasmic reticulum (ER) through the IP3R Ca^{2+} channels and to reduce the rate of intracellular Ca^{2+} efflux, evoking a lethal rise in $[Ca^{2+}]_i$.

Materials and methods

Materials. The Opti-MEM reduced serum media, fetal bovine serum, penicillin-streptomycin, Fura-2 AM, Fluo-4 AM, Mag-Fluo-4 AM, and the Annexin V-FITC staining Kit were from ThermoFisher Scientific (Burlington, ON, Canada). L-asparaginase (ASNase, ab73439) and 2,2-Bis(2-aminophenoxy)ethane-N,N,N',N'-tetraacetic acid tetrakis (acetoxymethyl ester) (BAPTA-AM) were from Abcam (Toronto, ON, Canada). 2,5-Di-tert-butylhydroquinone (TBHQ) and tetracaine (Tet) were from Sigma (Oakville, ON, Canada). Xestosponginc (XeC) was from Bio-Techne (Oakville, ON, Canada). Antibodies to OPRM1 (D-12), Bid (B-3), caspase-3 (E-8), caspase-12 (1611), poly(ADP-ribose) polymerase-1 (PARP1, F-2), GAPDH (0411), calpain-1 (6C-12), cytochrome C (H-104), voltage-dependent anion-selective channel 1 (VDAC-1, B-6), tubulin (D-10) and actin (I-19) were from Santa Cruz Biotech. (Dallas, TX, USA). The antibody against cleaved caspase-3 (D1-75) was from Cell Signaling (Whitby, ON). Trypan blue was from Life Technologies (Burlington, ON, Canada). Alamar blue was from Life Technologies (ON, Canada). Calpeptin was from Calbiochem, CA, USA.

Methods. We confirm that all methods described in this manuscript were carried out in accordance with relevant guidelines and regulations. All experiments followed the University of Calgary's biosafety guidelines.

Cell culture. POETIC2 parental cells (*) were derived from 14-year-old pre-B acute lymphoblastic leukemia patient. Generation of POETIC2 cells (*) stably infected with retrovirus carrying a pRS empty vector (*+pRS) or pRS-shOPRM1 (*+pRS-shOPRM1) was described previously³¹. POETIC 2 cells were cultured in Opti-MEM, containing 10% FBS and 100 μ g/ml penicillin-streptomycin, at 37 °C in 5% CO₂.

Determination of surviving cell population. Surviving population of cells (1×10^4 cells/well in 96 well plates) treated with different concentrations of D,L-methadone for 24 h were quantified using Alamar blue assay following the manufacturer's protocol.

Measurement of Ca^{2+} . (i) To measure resting $[Ca^{2+}]_i$, the method described by Grynkiewicz et al.³² was followed. Briefly, cells (5×10^5) loaded with 5 μ M Fluo-4 AM in Ca^{2+} -free KRH buffer at 37 °C for 30 min were washed with Ca^{2+} -free KRH buffer. Resting $[Ca^{2+}]_i$ was measured every 2 s at 485 nm excitation/530 nm emission using a Shimadzu RF 5301PC spectrofluorometer. F_{max} value was obtained after treatment with 0.02% saponin for 30 s and addition of 2 μ M $CaCl_2$ four times. F_{min} value was measured upon addition of 4 mM EDTA. $[Ca^{2+}]_i$ was calculated using the formula: free $[Ca^{2+}]_{cyt} = K_d [F - F_{min}] / [F_{max} - F]$ ³³, where K_d (for Fluo-4) = 345 nM. (ii) To measure ER Ca^{2+} release, cells (5×10^5) stably infected with retrovirus carrying a pRS empty vector or pRS-shOPRM1 were loaded with 2.5 μ M Mag-Fluo-4 AM for 30 min, washed with and resuspended in intracellular medium (ICM: 10 mM HEPES, pH 7.4, 19 mM NaCl, 125 mM KCl, 1 mM EGTA). ER Ca^{2+} release upon addition of increasing concentrations of D,L-methadone (0.25, 0.5 and 1 μ g/ml) \pm 2 μ M XeC or 1 mM Tet was

measured every 2 s using a Shimadzu RF 5301PC spectrofluorometer at $\lambda_{\text{ex}} = 495 \text{ nm}$ and $\lambda_{\text{em}} = 530 \text{ nm}$. (iii) To measure $[\text{Ca}^{2+}]_i$ transients by single cell Ca^{2+} imaging, cells grown in poly-L-ornithine-coated glass coverslips were loaded with 5 μM Fura-2 AM in Ca^{2+} -free Krebs–Ringer–Henseleit (KRH) buffer (25 mM HEPES, pH 7.4, 125 mM NaCl, 5 mM KCl, 6 mM glucose, 1.2 mM MgCl_2 and 2 μM EGTA), containing 0.02% Pluronic F-127 and 0.1 mg/ml BSA, for 20 min at room temperature. Coverslips were mounted in a perfusion chamber (Warner Instruments) and Ca^{2+} transients were analyzed by ratiometric single cell Ca^{2+} imaging while perfusing initially with Ca^{2+} -free KRH buffer for 3 min followed by buffer containing 0.5 $\mu\text{g/ml}$ D,L-methadone for 30 min then by buffer containing 5 μM TBHQ for 20 min. (iv) To measure Ca^{2+} entry and extrusion in cells loaded with 5 μM Fura-2 AM, internal Ca^{2+} stores were first vacated by treatment with 10 μM TBHQ in Ca^{2+} -free/EGTA-containing KRH buffer then treated with 0.5 $\mu\text{g/ml}$ D,L-methadone + 10 μM TBHQ, followed by repletion with 2 mM external Ca^{2+} to initiate Ca^{2+} entry. Where indicated, the buffer was switched to Ca^{2+} -free buffer containing 200 μM EGTA and 10 μM TBHQ to stop Ca^{2+} entry. $[\text{Ca}^{2+}]_i$ was monitored by capturing time lapse images every 5 s using Nikon TE2000-S inverted microscope, and analysis using the Compix Simple PCI 6 software³⁴. Fluorescence intensities were measured in individual cells ($n = 10$). Fura-2 filters have $\lambda_{\text{ex}} = 340 \pm 26$ and $387 \pm 11 \text{ nm}$ and $\lambda_{\text{em}} = 510 \pm 84 \text{ nm}$, and dichroic mirror (410 nm).

Western blot analysis. Cell lysates were analyzed by 12.5% SDS-PAGE and immunoblotting for PARP1, caspase-3, caspase-12, Bid, calpain 1 and actin. Immunoreactive bands were detected by enhanced chemiluminescence and visualized using the Bio-Rad ChemiDoc Imager at the optimal exposure setup. Ratios of protein bands of interest vs actin were determined after densitometry using the NIH ImageJ 1.61 software.

Analysis for apoptosis. POETIC2 cells (5×10^5) stably infected with retrovirus carrying a pRS empty vector or pRS-shOPRM1 were seeded in 6-cm dishes, pre-treated or untreated with 0.5 μM BAPTA-AM for 30 min, and treated with 0.5 $\mu\text{g/ml}$ D,L-methadone, 50 mIU L-asparaginase for 12 h. Cells were then harvested, washed twice with 1 \times PBS, stained with Annexin V-FITC (2 μl) and propidium iodide (2 μl), and analysed using an Attune NxT flow cytometer (ThermoFisher Scientific, USA).

Measurement of cytosolic cytochrome C level. Cytosolic and mitochondrial fractions were isolated as described previously³⁵. Briefly, cells were harvested by centrifugation at 370 \times g for 10 min, washed with 10 packed cell volumes of NKM buffer (1 mM Tris–HCl, pH 7.4, 0.13 M NaCl, 5 mM KCl and 7.5 mM MgCl_2) and resuspended in 6 packed cell volumes of homogenization buffer (10 mM Tris–HCl, pH 6.7, 10 mM KCl, 0.15 mM MgCl_2 , 1 mM PMSF and 1 mM DTT). Cells were then homogenized using a glass homogenizer (30 strokes), resuspended in 2 M sucrose solution and centrifuged at 1200 \times g for 5 min. The supernatant was subjected to further centrifugation at 7000 \times g for 10 min and the resulting supernatant was designated as cytosolic fraction. Pellets containing mitochondria were resuspend in 3 packed cell volumes of mitochondrial suspension buffer (10 mM Tris–HCl, pH 6.7, 0.15 mM MgCl_2 , 0.25 M sucrose, 1 mM PMSF and 1 mM DTT) and centrifuged at 10,000 \times g for 5 min. Pellets were designated as mitochondrial fraction. The cytosolic and mitochondrial fractions were analyzed by SDS-PAGE and immunoblotting for cytochrome C (cyt C), tubulin and VDAC-1. Ratios of cyt C vs tubulin or VDAC1 band intensities were determined after densitometry using NIH ImageJ 1.61. Standard deviations of the calculated ratios from three independent sets of experiments were determined.

Statistical analysis. Student's t-test (unpaired, two-tailed) was used. Significance was set at $p < 0.05$.

Results

D,L-Methadone induces leukemic cell apoptosis through activation of OPRM1. An opioid receptor has been implicated in D,L-methadone-induced leukemic cell apoptosis⁵, but the specific identity of this opioid receptor was not determined. Since we previously found that presence or absence of OPRM1 determines the fate of aLL cells following L-asparaginase treatment, i.e., presence leads to apoptosis while absence leads to survival or resistance³¹, we sought to examine the possibility that OPRM1 is targeted by D,L-methadone to induce leukemic cell apoptosis. To do so, we utilized POETIC2 cells (*) infected with retrovirus carrying a pRS empty vector (*+pRS) or pRS-shOPRM1 (*+pRS-shOPRM1) as model systems. POETIC2 cells are continuously growing leukemia cells established from a 14-year-old patient diagnosed with pre-B aLL³¹. As expected, OPRM1 loss in *+pRS-shOPRM1 cells (Fig. 1A) inhibited L-asparaginase-induced apoptosis (Fig. 1B, D; Supplementary Figs. 1 and 2). D,L-Methadone-induced apoptosis was also inhibited by loss of OPRM1 (Fig. 1C, D; Supplementary Figs. 1 and 2), indicating that D,L-methadone induces leukemic cell apoptosis through activation of OPRM1.

D,L-Methadone evokes Ca^{2+} release from internal stores, causing increased $[\text{Ca}^{2+}]_i$ that is inhibited by loss of OPRM1. D,L-Methadone was shown to induce leukemic cell death through stimulation of G_{opi} , reducing $[\text{cAMP}]_i$ and activating caspase-9 and -3⁵. However, in neurons, OPRM1 was implicated in intracellular Ca^{2+} homeostasis³⁶, perturbation of which can cause apoptosis. Thus, we aimed to determine whether D,L-methadone-induced apoptosis in leukemic cells is associated with altered $[\text{Ca}^{2+}]_i$. $[\text{Ca}^{2+}]_i$ is regulated by release of Ca^{2+} from internal stores, influx of extracellular Ca^{2+} , and extrusion of intracellular Ca^{2+} . Initial analysis for resting $[\text{Ca}^{2+}]_i$ revealed increased level in *+pRS cells compared to OPRM1-depleted *+pRS-shOPRM1 cells (Fig. 2A). We then examined whether D,L-methadone alters $[\text{Ca}^{2+}]_i$ through deregulation of Ca^{2+} release from internal stores. To do so, cells loaded with ratiometric Fura-2 AM were maintained in Ca^{2+} -free/EGTA-containing KRH buffer. By single-cell Ca^{2+} imaging, we found that D,L-methadone elicited a prompt increase in $[\text{Ca}^{2+}]_i$ in both *+pRS and *+pRS-shOPRM1 cells (Fig. 2B), suggesting that D,L-methadone stimulates

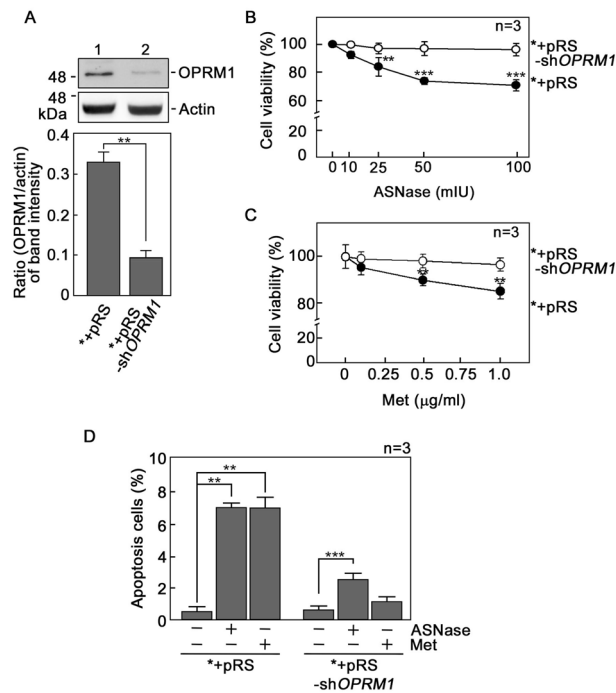


Figure 1. D,L-Methadone induces leukemic cell apoptosis through activation of OPRM1. (A) *OPRM1* depletion (upper panel) in POETIC2 leukemic cells (*) infected with retrovirus carrying pRS-sh*OPRM1* (*+pRS-sh*OPRM1*) but not in cells infected with retrovirus carrying an empty vector (*+pRS). Representative blots are from one of three independent experiments (n=3) showing similar results. Actin blot was used as loading control. The bottom panel shows the ratios of OPRM1 vs actin levels, which were measured by densitometric analysis of the blots using NIH ImageJ 1.61. Actin levels were normalized to 1.0. Standard deviation of the OPRM1 vs actin ratio was calculated from the three sets of experiments $**p < 0.0001$. (B) and (C) *+pRS-sh*OPRM1* cells exhibit resistance to L-asparaginase (ASNase: B) and D,L-methadone (Met: C). Cells were treated with increasing concentrations of L-asparaginase or D,L-methadone for 24 h and surviving cells were quantified using Alamar blue assay. Values are means \pm SEM from three independent experiments. $**p < 0.02$ and $***p < 0.001$. (D) L-asparaginase and D,L-methadone induce apoptosis in *+pRS cells, but OPRM1 loss in *+pRS-sh*OPRM1* cells inhibits L-asparaginase- and D,L-methadone-induced apoptosis. Flow cytometry analysis was performed in cells treated with 50 mIU ASNase or 0.5 μ g/ml Met for 12 h. Values are means \pm SEM from three independent experiments. $**p < 0.0001$ and $***p < 0.033$.

Ca^{2+} release from internal stores. However, the D,L-methadone-induced rise in $[Ca^{2+}]_i$ was reduced in *+pRS-sh*OPRM1* cells, indicating that the D,L-methadone-induced Ca^{2+} release from internal stores occurs via the OPRM1 pathway. Treatment with TBHQ³⁷, a potent inhibitor of the sarco/endoplasmic reticulum Ca^{2+} ATPase (SERCA) pump, triggered the release of internal Ca^{2+} stores, indicating that the *+pRS and *+pRS-sh*OPRM1* cells were viable during analysis.

D,L-Methadone evokes OPRM1-mediated Ca^{2+} release from the ER through the IP3R Ca^{2+} channel.

We next sought to determine whether the D,L-methadone-induced rise in $[Ca^{2+}]_i$ in leukemic cells is due to Ca^{2+} release from the ER. To do so, cells loaded with an ER Ca^{2+} probe³⁸, Mag-Fluo-4 AM, then treated with D,L-methadone were analyzed for ER Ca^{2+} release by spectrofluorometric Ca^{2+} imaging. As shown in Fig. 3A, D,L-methadone induced Ca^{2+} release from the ER but *+pRS-sh*OPRM1* cells showed reduced ER Ca^{2+} release compared to *+pRS cells, indicating inhibition of Ca^{2+} release by loss of OPRM1 and, therefore, D,L-methadone-induced ER Ca^{2+} release is mediated by OPRM1. We then tested whether D,L-methadone-induced ER Ca^{2+} release occurs through the IP3R and/or the ryanodine receptor (RyR), both of which form Ca^{2+} channels in the ER³⁹. For this experiment, Mag-Fluo-4 AM-loaded and D,L-methadone-stimulated cells were treated with xestospongin C (XeC, a potent IP3R inhibitor: Fig. 3B)⁴⁰ or tetracaine⁴¹ (Tet, a potent RyR inhibitor: Fig. 3C) and analyzed for ER Ca^{2+} release. As shown in Fig. 3, XeC (Fig. 3B) but not Tet (Fig. 3C) inhibited D,L-methadone-induced ER Ca^{2+} release, indicating that such Ca^{2+} release is mediated by IP3R and not by RyR.

The rate of Ca^{2+} extrusion following D,L-methadone treatment is slower in *+pRS cells compared to *+pRS-sh*OPRM1* cells. Our next step was to explore the possibility that OPRM1 loss also affects extracellular Ca^{2+} influx and intracellular Ca^{2+} extrusion following treatment with D,L-methadone. To do so, internal Ca^{2+} stores in Fura-2 AM-loaded cells were initially emptied by treatment with TBHQ in Ca^{2+} -free/EGTA-containing buffer. Cells were then treated with D,L-methadone in the presence of TBHQ followed by

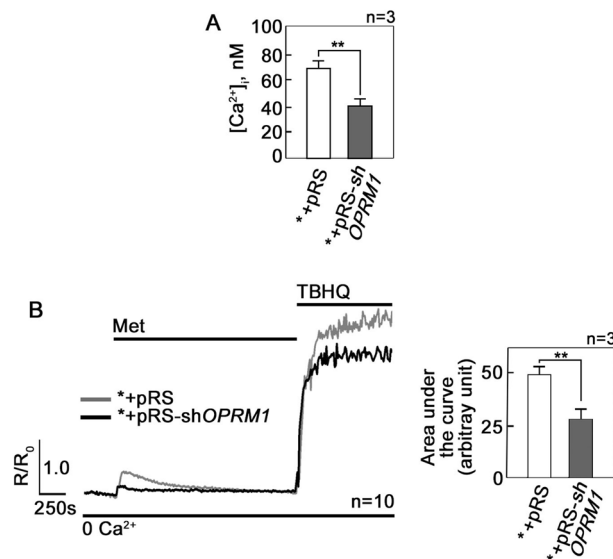


Figure 2. D,L-Methadone evokes Ca²⁺ release from internal stores, causing increased [Ca²⁺]_i that is inhibited by loss of OPRM1. **(A)** Resting [Ca²⁺]_i levels in *+pRS and *+pRS-shOPRM1 cells were measured as described in Materials and Methods. Values are means ± SEM from three independent experiments (n = 3). ***p* < 0.018. **(B)** Cells loaded with Fura-2 AM and treated with D,L-methadone were analyzed for Ca²⁺ transients in Ca²⁺-free buffer by ratiometric single-cell Ca²⁺ imaging using a Shimadzu RF 5301PC spectrofluorometer as described in Materials and Methods. Values represent means of Ca²⁺ signal traces in 10 cells from one of three independent experiments showing similar results (n = 3). Ca²⁺ response following TBHQ addition indicates that cells were viable during the assay. Analysis of the Ca²⁺ signal traces (left panel) indicates that D,L-methadone-induced increase in [Ca²⁺]_i is greater in *+pRS cells compared to *+pRS-shOPRM1 cells. Values are means ± SEM from three independent experiments (n = 3). ***p* < 0.025.

2 mM (Fig. 4A) or 500 mM Ca²⁺ (Supplementary Fig. 3), which was added to the external buffer to initiate Ca²⁺ entry. Ca²⁺ extrusion was also measured in the presence of TBHQ following a switch to Ca²⁺-free/EGTA-containing buffer. The initial treatment with TBHQ, which causes the release of internal Ca²⁺ stores, allows measurement of internal Ca²⁺ store capacity, and as shown in Fig. 4A, B, OPRM1-depleted *+pRS-shOPRM1 cells have reduced capacity compared to *+pRS cells. In the presence of D,L-methadone and upon external Ca²⁺ addition, there was no difference in Ca²⁺ entry between *+pRS and *+pRS-shOPRM1 cells (Fig. 4C) as well as in their rates of Ca²⁺ influx as measured by T_{1/2} of influx (Fig. 4D). However, upon switching to Ca²⁺-free/EGTA-containing buffer and withdrawal of D,L-methadone but continued presence of TBHQ, the rate of Ca²⁺ extrusion was faster (i.e., reduced T_{1/2} of efflux) in *+pRS-shOPRM1 cells compared to *+pRS cells (Fig. 4E), indicating that OPRM1 regulates the rate of Ca²⁺ extrusion. Thus, the integrated Ca²⁺ signals, which correspond to the calculated area under the curve [i.e., from the beginning to the end (back to baseline) of Ca²⁺ signal] was reduced in OPRM1-deficient *+pRS-shOPRM1 cells compared to control *+pRS cells (Fig. 4F).

D,L-Methadone-induced leukemic cell apoptosis is linked to increased [Ca²⁺]_i. Since we found that D,L-methadone, which causes leukemic cell apoptosis, triggers IP3R-mediated ER Ca²⁺ release and delays the rate of Ca²⁺ extrusion, causing increased [Ca²⁺]_i, we next wished to establish a link between the D,L-methadone-associated rise in [Ca²⁺]_i and D,L-methadone-induced apoptosis. Leukemic cells were treated with D,L-methadone in the presence or absence of the Ca²⁺ chelator, BAPTA-AM, then subjected to flow cytometry analysis after staining with PI and FITC-Annexin V. As shown in Fig. 5, D,L-methadone induced *+pRS cell apoptosis that was inhibited by BAPTA-AM, indicating that D,L-methadone-induced apoptosis is linked to increased [Ca²⁺]_i. Consistent with our results above, loss of OPRM1 in *+pRS-shOPRM1 cells inhibited D,L-methadone-induced apoptosis, which was unaffected by BAPTA-AM.

D,L-methadone induces leukemic cell apoptosis by upregulating the Ca²⁺-mediated calpain-1-Bid-cytochrome C-caspase-3/12 apoptotic pathway. Previously, D,L-methadone-induced leukemic cell apoptosis was linked to activation of caspase-9 and -3 as well as downregulation of BCL⁶. zVAD.fmk, the broad-spectrum inhibitor of caspases, almost completely inhibits D,L-methadone-induced leukemic cell apoptosis, indicating that caspases (together with BCL activation) is the main route for apoptosis. Here, we sought to analyze the expression of some of the components of the Ca²⁺-mediated apoptotic pathway in *+pRS leukemic cells treated with D,L-methadone. As shown in Fig. 6A, levels of activated calpain-1, t-Bid, caspase-3 and caspase-12 were elevated in D,L-methadone-treated *+pRS cells, and these were reversed by treatment with BAPTA-AM. A similar pattern was observed in the caspase-3-mediated PARP1 cleavage product. Inhibition of calpain-1 by calpeptin reduced D,L-methadone-induced leukemic cell apoptosis (Supplementary Fig. 4), indicat-

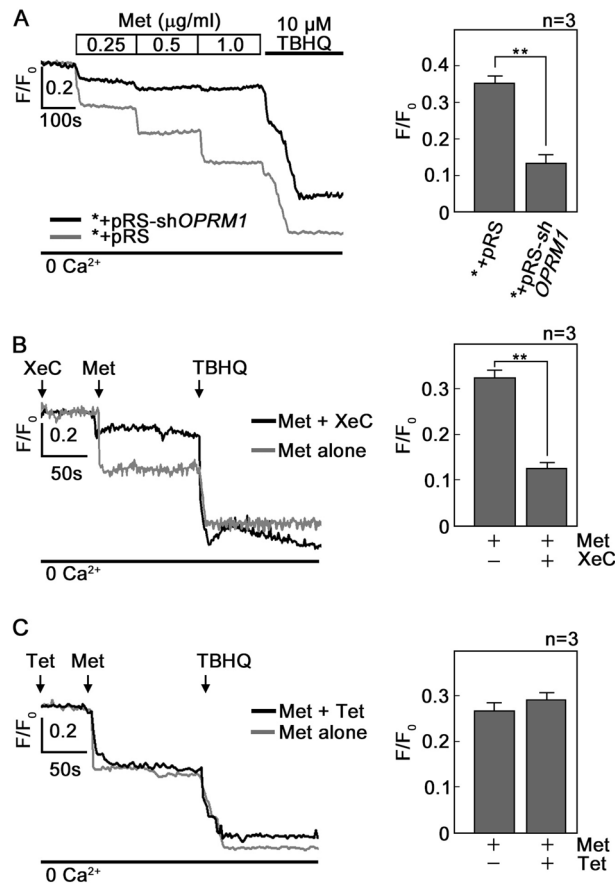


Figure 3. D,L-Methadone induces IP3R-mediated ER Ca²⁺ release that is inhibited by OPRM1 loss. (A) D,L-methadone induces ER Ca²⁺ release that is inhibited in OPRM1-depleted cells. *+pRS and *+pRS-shOPRM1 cells were loaded with Mag-Fluo-4 AM for 30 min then treated with increasing concentrations of D,L-methadone (0.25, 0.5 and 1 µg/ml) then analyzed for ER Ca²⁺ release by Ca²⁺ imaging. The chart on the right panel shows ER Ca²⁺ release upon treatment of cells with 0.5 µg/ml D,L-methadone. (B) and (C). D,L-Methadone-evoked ER Ca²⁺ release occurs via the IP3R channel. Thirty min after loading with Mag-Fluo-4 AM, *+pRS cells were treated with xestospongion C (XeC, in B) or tetracaine (Tet in C) for 10 min. ER Ca²⁺ release upon D,L-methadone addition was then measured every 2 s. The right panels show ER Ca²⁺ release upon treatment with D,L-methadone with or without prior treatment with XeC (B) or Tet (C). Representative data from one of three independent experiments (n = 3) showing similar results. Ca²⁺ response after TBHQ addition indicates that cells were viable during the assay. Values are means ± SEM from three independent experiments (n = 3). **p < 0.02.

ing the involvement of calpain-1 in D,L-methadone-induced leukemic cell apoptosis. As expected, translocation of t-Bid from the cytosol to mitochondria was observed (Fig. 6A, left and right bottom panels). Since activation of these elements of the Ca²⁺-mediated apoptotic pathway induces mitochondrial cytochrome c (cyt C) release into the cytosol, which leads to the activation of downstream caspases and subsequent apoptosis^{42,43}, we also examined cytosolic and mitochondrial cyt C levels in *+pRS cells following treatment with D,L-methadone. As shown in Fig. 6B, D,L-methadone caused an increase in cyt C level in the cytosol and corresponding decrease in mitochondria, which was reversed by BAPTA-AM treatment. We also assessed mPTP opening in D,L-methadone-induced leukemic cell apoptosis by calcein-AM staining followed by treatment with CoCl₂. Calcein-AM is a cell permeable fluorophore that diffuses and gets trapped in all subcellular compartments, including mitochondria. Treatment with cobalt (Co²⁺) quenches calcein fluorescence in all subcellular compartments except the mitochondrial matrix which is enclosed by a Co²⁺ impermeable inner mitochondrial membrane when mPTP is closed. Thus, the ability of Co²⁺ to quench mitochondrial calcein fluorescence only when mPTP is open allows determination of open vs closed status of mPTP in the cell. Upon treatment with CoCl₂, D,L-methadone treatment did not alter calcein fluorescence intensity, indicating that increased mPTP opening is not involved in D,L-methadone-induced apoptosis (Supplementary Fig. 5). Altogether, our findings support our view that D,L-methadone induces OPRM1-regulated apoptosis by increasing IP3R-mediated ER Ca²⁺ release and slowing down intracellular Ca²⁺ extrusion, causing a rise in [Ca²⁺]_i and upregulating the calpain-1-Bid-cytochrome C-caspase-3/12 apoptotic pathway.

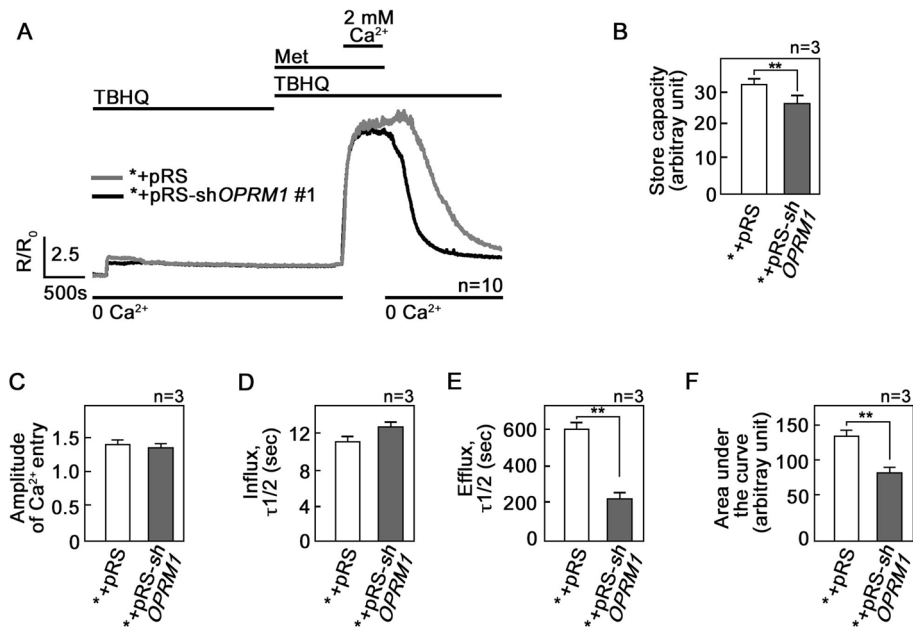


Figure 4. The rate of Ca²⁺ extrusion following D,L-methadone treatment in leukemic cells is accelerated by loss of OPRM1. (A) External Ca²⁺ entry and intracellular Ca²⁺ extrusion in +pRS and +pRS-shOPRM1 cells following D,L-methadone treatment. [Ca²⁺]_i was measured in cells loaded with Fura-2 AM and treated with TBHQ with or without D,L-methadone or external Ca²⁺ using single-cell Ca²⁺ imaging. Values represent means of Ca²⁺ signal traces from 10 cells. (B) Internal Ca²⁺ store capacity in OPRM1-depleted +pRS-shOPRM1 cells is reduced compared to that in control +pRS cells. Release of internal Ca²⁺ stores upon treatment with TBHQ allows measurement of internal Ca²⁺ store capacity. In the presence of D,L-methadone, there is no difference in (C) the amplitude of Ca²⁺ entry and (D) the rate of [Ca²⁺]_i influx in +pRS and +pRS-shOPRM1 cells. (E) The rate of Ca²⁺ extrusion, represented by the decline in [Ca²⁺]_i following removal of external Ca²⁺, is faster (i.e., reduced T_{1/2}) in +pRS-shOPRM1 cells than in +pRS cells. (F) Comparison of the integrated Ca²⁺ signals [area under the curve from the start of the Ca²⁺ signal (at 50 min) until 25 min later (at 75 min)] shows decreased Ca²⁺ transient in +pRS-shOPRM1 cells compared to +pRS cells. Values in (B)–(F) are means ± SEM from three independent experiments (n = 3). **p < 0.025.

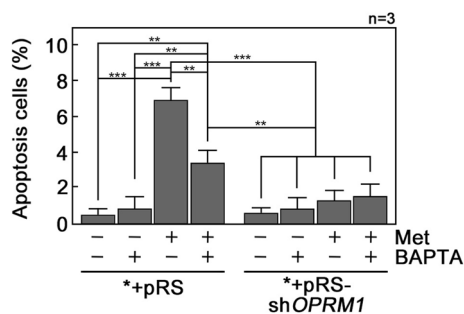


Figure 5. D,L-Methadone-induced apoptosis is reversed by Ca²⁺ chelation with BAPTA-AM. +pRS and +pRS-shOPRM1 cells pre-treated or untreated with 50 μM BAPTA-AM (BAPTA) for 30 min then treated or untreated with 0.5 μg/ml D,L-methadone for 12 h were stained with PI and FITC-Annexin V and subjected to flow cytometry as described in Materials and Methods. Values are means ± SEM from three independent experiments (n = 3). **p < 0.01 and ***p < 0.025.

Discussion

D,L-Methadone has recently been implicated in leukemic cell apoptosis^{4–6} and this pro-apoptotic effect has been linked to the opioid receptor signaling pathway⁵. In particular, D,L-methadone was found to induce apoptosis in HL-60 human myeloid leukemia and CEM human T-cell lymphoblastic leukemia cell lines via downregulation of both X chromosome-linked inhibitor of apoptosis (XIAP) and B-cell lymphoma-extra large (Bcl-x_L)⁴. In xenograft-derived aLL cells, it was reported that D,L-methadone induces apoptosis through activation of opioid GPCRs and subsequent downregulation of cAMP and activation of caspase-9 and -3⁵ (Fig. 7A). This was deduced from the observed expression of opioid receptors in leukemic cells and the inhibition of D,L-methadone-induced

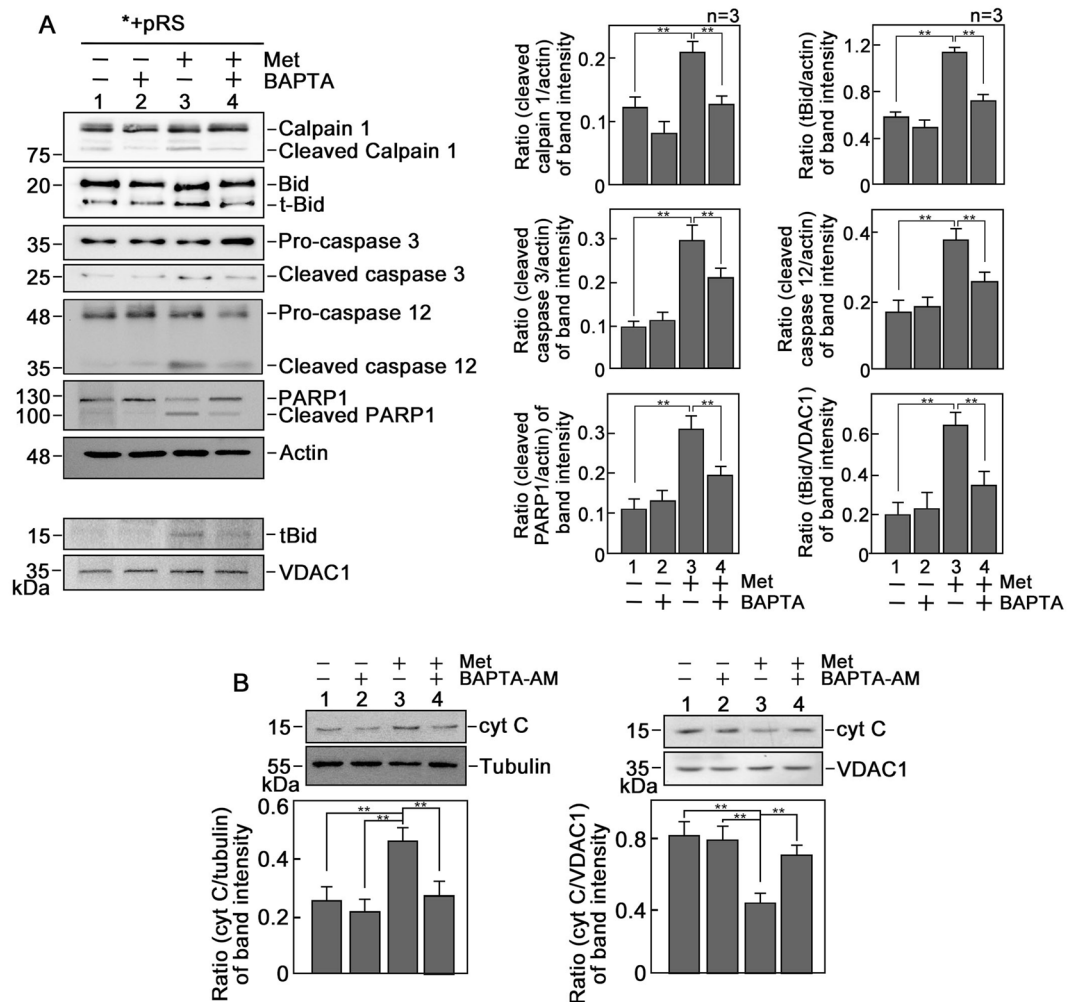


Figure 6. D,L-Methadone induces apoptosis through upregulation of the Ca^{2+} -mediated calpain-1-Bid-cytochrome C-caspase-3/12 apoptotic pathway. **(A)** Lysates of cells treated with D,L-methadone in the presence or absence of BAPTA-AM for 24 h were analyzed by SDS-PAGE and immunoblotting for calpain 1, Bid, caspase-3, cleaved caspase-3, caspase-12, PARP1 and actin. Actin blot was used as loading control. Mitochondrial fractions from cells treated as described above were also analyzed by SDS-PAGE and immunoblotting for t-Bid and VDAC1. Representative blots are from one of three independent experiments ($n=3$) showing similar results. Charts on the right panel show the ratios of the levels of apoptosis-associated proteins vs actin or VDAC1, with the actin and VDAC1 values normalized to 1.0. The charts correspond to the densitometry analysis of the representative blots shown on the left panel. **(B)** D,L-Methadone increases cytochrome C (cyt C) level in the cytosol. Cytosolic and mitochondrial fractions from cells pre-treated or untreated with $0.5 \mu\text{M}$ BAPTA-AM for 30 min then treated or untreated with $0.5 \mu\text{g/ml}$ D,L-methadone for 12 h were analyzed by SDS-PAGE and immunoblotting for cyt C, tubulin and VDAC1 (upper panels). Tubulin and VDAC1 were used as loading controls for cytosolic and mitochondrial fractions, respectively. Representative blots are from one of three independent experiments showing similar results. The lower panels show the ratios of cyt C vs tubulin or VDAC1 levels, with tubulin or VDAC1 levels normalized to 1.0. Values are means \pm SEM of the three independent experiments ($n=3$). $**p < 0.05$.

apoptosis by 3-isobutyl-1-methylxanthine (IBMX), PTX, and naloxone. IBMX is a cAMP phosphodiesterase inhibitor that causes cAMP upregulation; PTX inhibits the inhibitory α subunit ($G_{\alpha i}$) of heterotrimeric $G_{\alpha\beta\gamma}$ -proteins; and naloxone blocks opioid receptor activation. The indirect approach to ascertain opioid receptors as targets for D,L-methadone may, however, be questioned as the use of opioid receptor expression may be seen as a weak supporting evidence, and the use of naloxone appears to be challenged by reports that naloxone also inhibits toll-like receptor 4 (TLR4) signaling, a prominent regulator of immune cell function⁴⁴.

The current study utilized a stringent knockdown system to evaluate and identify OPRM1 as a specific D,L-methadone target that mediates apoptosis in leukemic cells. While it is believed that opioid receptors signal through $G_{\alpha i/o}$ subunits to inhibit adenylyl cyclase activity, reducing cAMP production and protein kinase A activity²², opioids elicit IP3R-mediated Ca^{2+} release from the ER via PLC^{45,46}. In leukocytes^{22,27}, pituitary²⁸ and neuroblastoma cells²⁶, $G_{\beta\gamma}$ subunit activation of PLC β and stimulation of IP3R are associated with opioid-induced

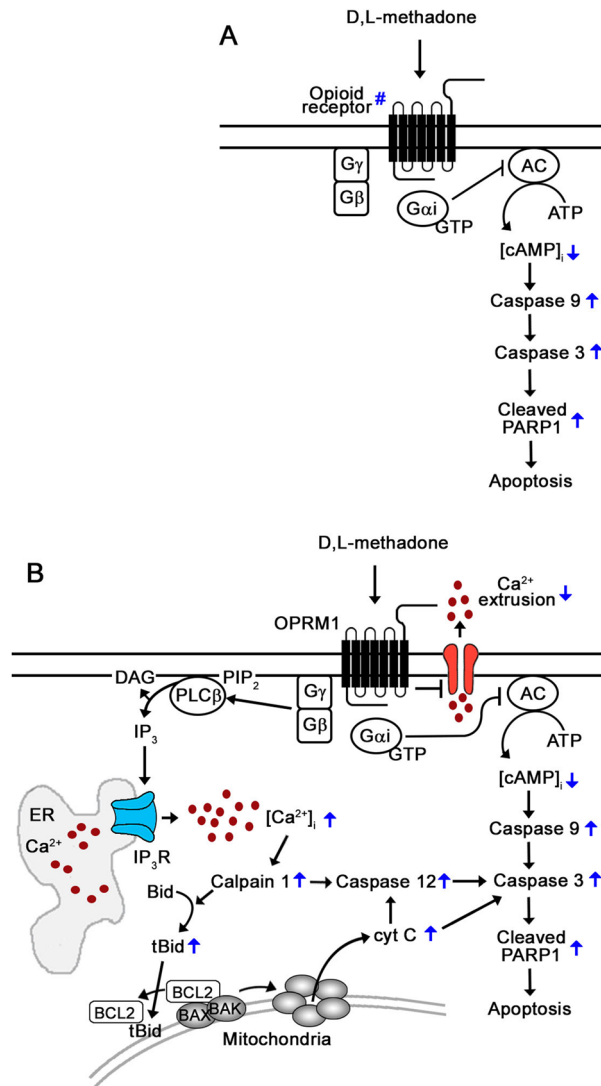


Figure 7. Proposed mechanism for OPRM1-mediated D,L-methadone-induced apoptosis in leukemic cells. **(A)** Previously, stimulation of an unidentified type of opioid receptor (#) by D,L-methadone was shown to induce leukemic cell death via $G_{\alpha i}$, which blocks adenylyl cyclase activity that in turn reduces $[cAMP]_i$, activating caspase-9 and -3⁵. **(B)** In the current study, we identify the OPRM1 opioid receptor as a specific D,L-methadone target in leukemic cells. Since activation of opioid receptors has been shown to cause $G_{\beta\gamma}$ -mediated rise in $[Ca^{2+}]_i$ via PLC^{22,26–28}, we propose that D,L-methadone activation of OPRM1 in leukemic cells causes $G_{\beta\gamma}$ -mediated stimulation of PLC, which then triggers a rise in $[Ca^{2+}]_i$ through increased IP3R-mediated ER Ca^{2+} release and reduced rate of Ca^{2+} efflux, causing upregulation of the Ca^{2+} -mediated calpain-1-Bid-cyt C-caspase-3/12 apoptotic pathway and subsequent apoptosis.

increase in $[Ca^{2+}]_i$. Similarly, mu-opioid receptor-mediated PLC activation through a PTX-sensitive G protein and possible IP3-mediated increase in $[Ca^{2+}]_i$ in neuroblastoma cells were presumed to be involved in opioid action²⁹. These findings together with our previous discovery that aLL cell expression of OPRM1 leads to apoptosis following L-asparaginase treatment while lack of OPRM1 expression leads to survival or resistance to L-asparaginase³¹, prompted us to investigate the possibility that OPRM1 is targeted by D,L-methadone to induce leukemic cell apoptosis, and that OPRM1 regulation of $[Ca^{2+}]_i$ is a critical component of D,L-methadone-induced apoptotic pathway in leukemic cells.

Our studies revealed that resting $[Ca^{2+}]_i$ in control *+pRS leukemic cells is increased compared to OPRM1-depleted *+pRS-shOPRM1 cells. We established that increased $[Ca^{2+}]_i$ in *+pRS cells is linked to the stimulation of apoptosis by D,L-methadone, and that the rise in $[Ca^{2+}]_i$ is due to increased IP3R-mediated ER Ca^{2+} release and reduced rate of intracellular Ca^{2+} extrusion. These conclusions were based on the analysis of cells treated with the Mag-Fluo-4 AM Ca^{2+} probe³⁸, which distinguishes the release of Ca^{2+} from the ER, and with XeC, which inhibits Ca^{2+} release via the IP3R Ca^{2+} channel⁴⁰, as well as by introduction and withdrawal of extracellular Ca^{2+} in the presence of TBHQ, which empties internal Ca^{2+} stores³⁷, allowing measurement of intracellular Ca^{2+} extrusion. These observed Ca^{2+} dynamics in *+pRS cells following treatment with D,L-methadone are reversed by loss of

OPRM1. Apparently, while D,L-methadone induces ER Ca²⁺ release and delays Ca²⁺ efflux in *+pRS cells, causing a lethal rise in [Ca²⁺]_i, loss of OPRM1 in *+pRS-shOPRM1 cells inhibits ER Ca²⁺ release and accelerates Ca²⁺ efflux following D,L-methadone treatment, preventing a lethal rise in [Ca²⁺]_i, and subsequently inhibiting D,L-methadone-induced apoptosis. Thus, our findings support an OPRM1-regulated D,L-methadone-induced [Ca²⁺]_i-mediated apoptotic pathway in leukemic cells.

In fact, we demonstrate that OPRM1-regulated Ca²⁺-mediated apoptosis induced by D,L-methadone in leukemic cells is triggered by activation of the Ca²⁺-dependent calpain-1 and associated proteolytic events mediated by cysteine proteases. Our findings are consistent with the model illustrated in Fig. 7B where Ca²⁺-activated calpain-1 targets Bid to generate its truncated form, t-Bid, which translocates to mitochondria where it binds and neutralizes the anti-apoptotic Bcl-2. This allows BAK and BAX to form pores in the outer mitochondrial membrane, causing cyt C release, activation of caspases such as caspase-12⁴⁷ and caspase-3⁴⁸, and subsequent apoptosis^{42,43,49}. Caspase-3 cleaves PARP1, which drives apoptosis in leukemic cells⁵⁰. Our analysis show that D,L-methadone triggers OPRM1-regulated apoptosis by inducing cleavage of calpain-1, Bid, procaspase-3, procaspase-12 and PARP1, indicating an [Ca²⁺]_i-mediated apoptosis. This was substantiated by the reversal of apoptosis by the Ca²⁺ chelator, BAPTA-AM.

In summary, we identify OPRM1 as a novel and specific D,L-methadone target in leukemic cells. Our observations indicate that D,L-methadone activates OPRM1, which triggers an increase in IP3R-mediated ER Ca²⁺ release and decrease in the rate of Ca²⁺ efflux, causing a rise in [Ca²⁺]_i that upregulates the Ca²⁺-mediated calpain-1-Bid-cyt C-caspase-3/12 apoptotic pathway. We note that although loss of OPRM1 in *+pRS-shOPRM1 cells almost completely inhibited D,L-methadone-induced apoptosis, indicating that D,L-methadone primarily targets OPRM1 to induce leukemic cell death, the fact that BAPTA-AM only partially inhibits D,L-methadone-induced *+pRS cell apoptosis suggests the co-existence of at least one other branch of the OPRM1-mediated D,L-methadone-induced apoptotic pathway. While still under our separate investigation, we presume that the previously reported D,L-methadone-induced apoptotic pathway that downregulates cAMP is in fact a branch of the OPRM1 apoptotic pathway. Certainly, the mode of action of D,L-methadone requires further investigation if it is to be clinically deliberated as a relevant adjuvant or sensitizer for aLL chemotherapy.

Received: 30 July 2020; Accepted: 22 December 2020

Published online: 13 January 2021

References

- Capria, S. *et al.* A review of current induction strategies and emerging prognostic factors in the management of children and adolescents with acute lymphoblastic leukemia. *Expert Rev. Hematol.* <https://doi.org/10.1080/17474086.2020.1770591> (2020).
- Hunger, S. P. & Mullighan, C. G. Acute lymphoblastic leukemia in children. *N. Engl. J. Med.* **373**, 1541–1552. <https://doi.org/10.1056/NEJMra1400972> (2015).
- Thomas, X. & Le Jeune, C. Treating adults with acute lymphocytic leukemia: New pharmacotherapy options. *Expert Opin. Pharmacother.* **17**, 2319–2330. <https://doi.org/10.1080/14656566.2016.1250884> (2016).
- Friesen, C., Bacher, S., Hormann, I., Roscher, M. & Miltner, E. Cytotoxic effects of opioids on cancer cell lines. *Int. J. Clin. Pharmacol. Ther.* **49**, 60–62 (2011).
- Friesen, C. *et al.* Cell death sensitization of leukemia cells by opioid receptor activation. *Oncotarget* **4**, 677–690. <https://doi.org/10.18632/oncotarget.952> (2013).
- Friesen, C., Roscher, M., Alt, A. & Miltner, E. Methadone, commonly used as maintenance medication for outpatient treatment of opioid dependence, kills leukemia cells and overcomes chemoresistance. *Cancer Res.* **68**, 6059–6064. <https://doi.org/10.1158/0008-5472.CAN-08-1227> (2008).
- Friesen, C. *et al.* Opioid receptor activation triggering downregulation of cAMP improves effectiveness of anti-cancer drugs in treatment of glioblastoma. *Cell Cycle* **13**, 1560–1570. <https://doi.org/10.4161/cc.28493> (2014).
- Fishman, S. M., Wilsey, B., Mahajan, G. & Molina, P. Methadone reincarnated: Novel clinical applications with related concerns. *Pain Med* **3**, 339–348. <https://doi.org/10.1046/j.1526-4637.2002.02047.x> (2002).
- Fredheim, O. M., Moksnes, K., Borchgrevink, P. C., Kaasa, S. & Dale, O. Clinical pharmacology of methadone for pain. *Acta Anaesthesiol. Scand.* **52**, 879–889. <https://doi.org/10.1111/j.1399-6576.2008.01597.x> (2008).
- Yin, D., Mufson, R. A., Wang, R. & Shi, Y. Fas-mediated cell death promoted by opioids. *Nature* **397**, 218. <https://doi.org/10.1038/16612> (1999).
- Li, Y. *et al.* Toll-like receptor 2 is required for opioids-induced neuronal apoptosis. *Biochem Biophys. Res. Commun.* **391**, 426–430. <https://doi.org/10.1016/j.bbrc.2009.11.074> (2010).
- Xiao, Y., Smith, R. D., Caruso, F. S. & Kellar, K. J. Blockade of rat alpha3beta4 nicotinic receptor function by methadone, its metabolites, and structural analogs. *J. Pharmacol. Exp. Ther.* **299**, 366–371 (2001).
- Gorman, A. L., Elliott, K. J. & Inturrisi, C. E. The D- and L-isomers of methadone bind to the non-competitive site on the N-methyl-D-aspartate (NMDA) receptor in rat forebrain and spinal cord. *Neurosci. Lett.* **223**, 5–8. [https://doi.org/10.1016/s0304-3940\(97\)13391-2](https://doi.org/10.1016/s0304-3940(97)13391-2) (1997).
- Kristensen, K., Christensen, C. B. & Christrup, L. L. The mu1, mu2, delta, kappa opioid receptor binding profiles of methadone stereoisomers and morphine. *Life Sci.* **56**, PL45–PL50. [https://doi.org/10.1016/0024-3205\(94\)00426-s](https://doi.org/10.1016/0024-3205(94)00426-s) (1995).
- Regan, P. M., Langford, D. & Khalili, K. Regulation and functional implications of opioid receptor splicing in opioid pharmacology and HIV pathogenesis. *J. Cell Physiol.* **231**, 976–985. <https://doi.org/10.1002/jcp.25237> (2016).
- Pan, Y. X. Diversity and complexity of the mu opioid receptor gene: alternative pre-mRNA splicing and promoters. *DNA Cell Biol.* **24**, 736–750. <https://doi.org/10.1089/dna.2005.24.736> (2005).
- Al-Hasani, R. & Bruchas, M. R. Molecular mechanisms of opioid receptor-dependent signaling and behavior. *Anesthesiology* **115**, 1363–1381. <https://doi.org/10.1097/ALN.0b013e318238bba6> (2011).
- Predescu, D. V. *et al.* G protein-coupled receptors (GPCRs)-mediated calcium signaling in ovarian cancer: Focus on GPCRs activated by neurotransmitters and inflammation-associated molecules. *Int. J. Mol. Sci.* <https://doi.org/10.3390/ijms20225568> (2019).
- Jordan, B. & Devi, L. A. Molecular mechanisms of opioid receptor signal transduction. *Br. J. Anaesth.* **81**, 12–19. <https://doi.org/10.1093/bja/81.1.12> (1998).
- Law, P. Y. in *The Opiate Receptors* (ed G. W. Pasternak) 195–238 (Humana Press, 2011).
- Hsia, J. A., Moss, J., Hewlett, E. L. & Vaughan, M. ADP-ribosylation of adenylate cyclase by pertussis toxin. Effects on inhibitory agonist binding. *J. Biol. Chem.* **259**, 1086–1090 (1984).

22. Machelska, H. & Celik, M. O. Advances in achieving opioid analgesia without side effects. *Front. Pharmacol.* **9**, 1388. <https://doi.org/10.3389/fphar.2018.01388> (2018).
23. Seamon, K. B., Padgett, W. & Daly, J. W. Forskolin: Unique diterpene activator of adenylate cyclase in membranes and in intact cells. *Proc. Natl. Acad. Sci. USA* **78**, 3363–3367. <https://doi.org/10.1073/pnas.78.6.3363> (1981).
24. Law, P. Y., Wong, Y. H. & Loh, H. H. Molecular mechanisms and regulation of opioid receptor signaling. *Annu. Rev. Pharmacol. Toxicol.* **40**, 389–430. <https://doi.org/10.1146/annurev.pharmtox.40.1.389> (2000).
25. Chan, J. S., Chiu, T. T. & Wong, Y. H. Activation of type II adenylyl cyclase by the cloned mu-opioid receptor: Coupling to multiple G proteins. *J. Neurochem.* **65**, 2682–2689. <https://doi.org/10.1046/j.1471-4159.1995.65062682.x> (1995).
26. Yoon, S. H., Lo, T. M., Loh, H. H. & Thayer, S. A. Delta-opioid-induced liberation of Gbetagamma mobilizes Ca²⁺ stores in NG108-15 cells. *Mol. Pharmacol.* **56**, 902–908. <https://doi.org/10.1124/mol.56.5.902> (1999).
27. Celik, M. O. *et al.* Leukocyte opioid receptors mediate analgesia via Ca(2+)-regulated release of opioid peptides. *Brain Behav. Immun.* **57**, 227–242. <https://doi.org/10.1016/j.bbi.2016.04.018> (2016).
28. Charles, A. C. *et al.* Coexpression of delta-opioid receptors with micro receptors in GH3 cells changes the functional response to micro agonists from inhibitory to excitatory. *Mol. Pharmacol.* **63**, 89–95. <https://doi.org/10.1124/mol.63.1.89> (2003).
29. Smart, D., Smith, G. & Lambert, D. G. mu-Opioid receptor stimulation of inositol (1,4,5)trisphosphate formation via a pertussis toxin-sensitive G protein. *J. Neurochem.* **62**, 1009–1014. <https://doi.org/10.1046/j.1471-4159.1994.62031009.x> (1994).
30. Orlov, S. N. *et al.* Activation of cAMP signaling transiently inhibits apoptosis in vascular smooth muscle cells in a site upstream of caspase-3. *Cell Death Differ.* **6**, 661–672. <https://doi.org/10.1038/sj.cdd.4400539> (1999).
31. Kang, S. M. *et al.* Genome-wide loss-of-function genetic screening identifies opioid receptor mu1 as a key regulator of L-asparaginase resistance in pediatric acute lymphoblastic leukemia. *Oncogene* **36**, 5910–5913. <https://doi.org/10.1038/ncr.2017.211> (2017).
32. Grynkiewicz, G., Poenie, M. & Tsien, R. Y. A new generation of Ca²⁺ indicators with greatly improved fluorescence properties. *J. Biol. Chem.* **260**, 3440–3450 (1985).
33. Kaufmann, R., Mussbach, F., Henklein, P. & Settmacher, U. Proteinase-activated receptor 2-mediated calcium signaling in hepatocellular carcinoma cells. *J. Cancer. Res. Clin. Oncol.* **137**, 965–973. <https://doi.org/10.1007/s00432-010-0961-1> (2011).
34. Liu, Y. *et al.* Roles of the NH2-terminal domains of cardiac ryanodine receptor in Ca²⁺ release activation and termination. *J. Biol. Chem.* **290**, 7736–7746. <https://doi.org/10.1074/jbc.M114.618827> (2015).
35. Kiss, D. S. *et al.* Preparation of purified perikaryal and synaptosomal mitochondrial fractions from relatively small hypothalamic brain samples. *MethodsX* **3**, 417–429. <https://doi.org/10.1016/j.mex.2016.05.004> (2016).
36. Whistler, J. L., Chuang, H. H., Chu, P., Jan, L. Y. & von Zastrow, M. Functional dissociation of mu opioid receptor signaling and endocytosis: Implications for the biology of opiate tolerance and addiction. *Neuron* **23**, 737–746. [https://doi.org/10.1016/s0896-6273\(01\)80032-5](https://doi.org/10.1016/s0896-6273(01)80032-5) (1999).
37. Jan, C. R., Ho, C. M., Wu, S. N. & Tseng, C. J. Mechanism of rise and decay of 2,5-di-tert-butylhydroquinone-induced Ca²⁺ signals in Madin Darby canine kidney cells. *Eur. J. Pharmacol.* **365**, 111–117. [https://doi.org/10.1016/s0014-2999\(98\)00871-1](https://doi.org/10.1016/s0014-2999(98)00871-1) (1999).
38. Takahashi, A., Camacho, P., Lechleiter, J. D. & Herman, B. Measurement of intracellular calcium. *Physiol. Rev.* **79**, 1089–1125. <https://doi.org/10.1152/physrev.1999.79.4.1089> (1999).
39. Go, L. O. *et al.* Differential regulation of two types of intracellular calcium release channels during end-stage heart failure. *J. Clin. Invest.* **95**, 888–894. <https://doi.org/10.1172/JCI117739> (1995).
40. Solanes, P. *et al.* Space exploration by dendritic cells requires maintenance of myosin II activity by IP3 receptor 1. *EMBO J.* **34**, 798–810. <https://doi.org/10.15252/emboj.201489056> (2015).
41. Westcott, E. B., Goodwin, E. L., Segal, S. S. & Jackson, W. F. Function and expression of ryanodine receptors and inositol 1,4,5-trisphosphate receptors in smooth muscle cells of murine feed arteries and arterioles. *J. Physiol.* **590**, 1849–1869. <https://doi.org/10.1113/jphysiol.2011.222083> (2012).
42. Takano, J. *et al.* Calpain mediates excitotoxic DNA fragmentation via mitochondrial pathways in adult brains: evidence from calpastatin mutant mice. *J. Biol. Chem.* **280**, 16175–16184. <https://doi.org/10.1074/jbc.M414552200> (2005).
43. Wang, K., Yin, X. M., Chao, D. T., Milliman, C. L. & Korsmeyer, S. J. BID: A novel BH3 domain-only death agonist. *Genes Dev.* **10**, 2859–2869. <https://doi.org/10.1101/gad.10.22.2859> (1996).
44. Hutchinson, M. R. *et al.* Non-stereoselective reversal of neuropathic pain by naloxone and naltrexone: Involvement of toll-like receptor 4 (TLR4). *Eur. J. Neurosci.* **28**, 20–29. <https://doi.org/10.1111/j.1460-9568.2008.06321.x> (2008).
45. Sarne, Y. & Gafni, M. Determinants of the stimulatory opioid effect on intracellular calcium in SK-N-SH and NG108-15 neuroblastoma. *Brain Res.* **722**, 203–206. [https://doi.org/10.1016/0006-8993\(96\)00191-6](https://doi.org/10.1016/0006-8993(96)00191-6) (1996).
46. Jin, W., Lee, N. M., Loh, H. H. & Thayer, S. A. Opioids mobilize calcium from inositol 1,4,5-trisphosphate-sensitive stores in NG108-15 cells. *J. Neurosci.* **14**, 1920–1929 (1994).
47. Harwood, S. M., Yaqoob, M. M. & Allen, D. A. Caspase and calpain function in cell death: Bridging the gap between apoptosis and necrosis. *Ann. Clin. Biochem.* **42**, 415–431. <https://doi.org/10.1258/000456305774538238> (2005).
48. Mandic, A. *et al.* Calpain-mediated Bid cleavage and calpain-independent Bak modulation: Two separate pathways in cisplatin-induced apoptosis. *Mol. Cell Biol.* **22**, 3003–3013. <https://doi.org/10.1128/mcb.22.9.3003-3013.2002> (2002).
49. Gavathiotis, E. *et al.* BAX activation is initiated at a novel interaction site. *Nature* **455**, 1076–1081. <https://doi.org/10.1038/nature07396> (2008).
50. Diamantopoulos, P. T. *et al.* PARP1-driven apoptosis in chronic lymphocytic leukemia. *Biomed. Res. Int.* **2014**, 106713. <https://doi.org/10.1155/2014/106713> (2014).

Acknowledgements

This work was supported by a grant from NSERC (RGPIN/06270-2019) to KYL.

Author contributions

J.K.L. performed all the experiments and wrote a draft of the manuscript. H.G.B. contributed to experimental design. K.Y.L. and J.L.R. contributed to the analysis and interpretation of data and/or experimental design. J.L.R. and K.Y.L. critically revised the manuscript for important intellectual content and wrote the final version of the manuscript.

Competing interests

The authors declare no competing interests.

Additional information

Supplementary Information The online version contains supplementary material available at <https://doi.org/10.1038/s41598-020-80520-w>.

Correspondence and requests for materials should be addressed to K.-Y.L.

Reprints and permissions information is available at www.nature.com/reprints.

Publisher's note Springer Nature remains neutral with regard to jurisdictional claims in published maps and institutional affiliations.



Open Access This article is licensed under a Creative Commons Attribution 4.0 International License, which permits use, sharing, adaptation, distribution and reproduction in any medium or format, as long as you give appropriate credit to the original author(s) and the source, provide a link to the Creative Commons licence, and indicate if changes were made. The images or other third party material in this article are included in the article's Creative Commons licence, unless indicated otherwise in a credit line to the material. If material is not included in the article's Creative Commons licence and your intended use is not permitted by statutory regulation or exceeds the permitted use, you will need to obtain permission directly from the copyright holder. To view a copy of this licence, visit <http://creativecommons.org/licenses/by/4.0/>.

© The Author(s) 2021